Block-Level Interference Exploitation Precoding without Symbol-by-Symbol Optimization

Ang Li*, Chao Shen[‡], Xuewen Liao*, Christos Masouros[†], and A. Lee Swindlehurst[¶]
School of Information and Communications Engineering, Xi'an Jiaotong University, Xi'an, China*
Shenzhen Research Institute of Big Data, Shenzhen, China[‡]
Department of Electronic and Electrical Engineering, University College London, London, UK[†]
Center for Pervasive Communications and Computing, University of California, Irvine, USA[¶]
Email: {ang.li.2020, yeplos}@xjtu.edu.cn*, chaoshen@sribd.cn[‡], c.masouros@ucl.ac.uk[†], swindle@uci.edu[¶]

Abstract—Symbol-level precoding (SLP) based on the concept of constructive interference (CI) is shown to be superior to traditional block-level precoding (BLP), however at the cost of a symbol-by-symbol optimization during the precoding design. In this paper, we propose a CI-based block-level precoding (CI-BLP) scheme for the downlink transmission of a multi-user multipleinput single-output (MU-MISO) communication system, where we design a constant precoding matrix to a block of symbol slots to exploit CI for each symbol slot simultaneously. A single optimization problem is formulated to maximize the minimum CI effect over the entire block, thus reducing the computational cost of traditional SLP as the optimization problem only needs to be solved once per block. By leveraging the Karush-Kuhn-Tucker (KKT) conditions and the dual problem formulation, the original optimization problem is finally shown to be equivalent to a quadratic programming (QP) over a simplex. Numerical results validate our derivations and exhibit superior performance for the proposed CI-BLP scheme over traditional BLP and SLP methods, thanks to the relaxed block-level power constraint.

Index Terms—MIMO, symbol-level precoding, constructive interference, interference exploitation, optimization.

I. INTRODUCTION

Interference management plays a crucial role for reliable communication in multiple-input multiple-output (MIMO) systems. In the downlink transmission of a multi-user MIMO system, precoding is essential for realizing spatial multiplexing, and a number of block-level precoding (BLP) approaches have been designed in the literature to manage multi-user interference. This includes zero-forcing (ZF) precoding [1] and block-diagonalization (BD) precoding [2], as well as the regularized ZF (RZF) precoding that enhances the performance of ZF precoding [3]. Furthermore, optimization-based precoding schemes have been proposed in the literature for additional performance improvements over closed-form precoders, for example the signal-to-interference-plus-noise ratio (SINR) balancing precoding [4], [5], and the weighted minimum mean-squared error (W-MMSE) precoder [6].

More recently, the concept of constructive interference (CI) has been introduced to the precoder design in MIMO commu-

This work is supported in part by the Young Elite Scientists Sponsorship Program by CIC (Grant No. 2021QNRC001), in part by the National Natural Science Foundation of China under Grant 62101422, in part by the Science and Technology Program of Shaanxi Province under Grant 2021KWZ-01, and in part by the Fundamental Research Funds for the Central Universities under Grant xzy012020007.

nications [7], [8], where it is shown that by further exploiting the data symbol information in addition to the channel state information (CSI), instantaneous interference existing in multiuser transmission can be categorized into constructive and destructive, and judicious precoding approaches have been designed to exploit the constructive part of multi-user interference and meanwhile transform the destructive part into constructive, leading to significant performance improvements [9], [10]. However, it should be mentioned that the performance benefits of CI-based precoding come at the cost of a symbolby-symbol design methodology, i.e., symbol-level precoding (SLP) where the precoder must be designed for each symbol slot is required. This poses a significant computational burden on the multi-user MIMO communication system, because the base station (BS) needs to solve an independent optimization problem for each symbol slot. To alleviate the computational costs, several studies attempt to reduce the complexity of the CI-SLP optimization problem, including derivations of the optimal precoding structure for CI-SLP with efficient iterative algorithms [10], sub-optimal solutions [11], blocklevel optimization attempts [12], [13], and deep learning-based methods [14]. Despite the above attempts, most of the above approaches still require solving the problem at symbol level, i.e., the total number of CI-SLP problems that must be solved in a channel coherence interval is however not reduced.

In this paper, we propose a CI-based block-level precoding (CI-BLP) approach that applies a constant precoding matrix to a block of symbol slots in a downlink multi-user multiple-input single-output (MU-MISO) system, where CI is achieved for all the symbol slots of the transmission block simultaneously. Based on the 'symbol-scaling' CI metric, a single optimization problem is formulated to maximize the minimum CI effect over all symbol slots subject to a block- rather than symbollevel power budget. By leveraging the Lagrangian method and studying the corresponding dual problem, the original CI-BLP optimization problem is finally shown to be equivalent to a QP optimization over a simplex. Numerical results demonstrate that the proposed CI-BLP approach offers an improved error-rate performance compared with traditional CI-SLP approaches thanks to the relaxed block-level power constraint, which meanwhile require fewer computational costs as the optimization problem only needs to be solved once per block.

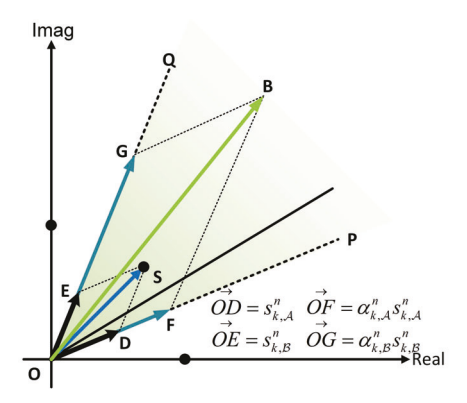


Fig. 1: An illustration for 'symbol-scaling' CI metric, 8PSK

II. SYSTEM MODEL AND CONSTRUCTIVE INTERFERENCE A. System Model

The downlink transmission of a MU-MISO communication system is considered, where a total number of K single-antenna users are served by a BS with $N_{\rm T}$ transmit antennas, and $K \leq N_{\rm T}$. We focus on the transmission of a block of symbol slots, where we introduce $\mathbf{s}^n = \left[s_1^n, s_2^n, \cdots, s_K^n\right]^{\rm T} \in \mathbb{C}^{K \times 1}$ as the data symbol vector in the n-th slot, drawn from normalized PSK constellations. Accordingly, the received signal for user k in the n-th symbol slot can be expressed as

$$y_k^n = \mathbf{h}_k^{\mathrm{T}} \mathbf{W} \mathbf{s}^n + z_k^n, \tag{1}$$

where $\mathbf{h}_k \in \mathbb{C}^{N_{\mathrm{T}} \times 1}$ represents the channel vector between the transmit antenna array and the k-th user¹, which is constant within the considered block, and z_k^n is additive Gaussian noise with zero mean and variance σ^2 . $\mathbf{W} \in \mathbb{C}^{N_{\mathrm{T}} \times K}$ is the precoding matrix that applies to all \mathbf{s}^n in the block.

B. Constructive Interference

CI is the interference that is able to push the signals of interest further away from the decision boundaries of their modulated symbol constellation, such that the received signals have a higher probability to be correctly detected [7]. In this paper, we employ the 'symbol-scaling' CI metric for PSK modulation to ease our subsequent derivations [15]. To illustrate the concept of the 'symbol-scaling' CI metric, in Fig. 1 we depict one quarter of a 8PSK constellation as an example, where without loss of generality we denote $OS = s_k^n$ as the data symbol of interest for user k in the n-th symbol slot, and $\overrightarrow{OB} = \mathbf{h}_k^{\mathrm{T}} \mathbf{W} \mathbf{s}^n$ as the corresponding received signal excluding noise. The 'symbol-scaling' CI metric decomposes the data symbols and the received signals along their corresponding decision boundaries, i.e., $\overrightarrow{OS} = \overrightarrow{OD} + \overrightarrow{OE}$ and $\overrightarrow{OB} = \overrightarrow{OF} + \overrightarrow{OG}$. To obtain a better error-rate performance, CI precoding aims to push the received signal OB further away from the decision boundaries $(\overrightarrow{OP} \text{ and } \overrightarrow{OQ} \text{ in Fig. 1})$, and this is equivalent to increasing the amplitude for \overrightarrow{OF} and \overrightarrow{OG} as much as possible, as will be shown in Section III-A mathematically.

¹Since we focus on deriving the optimal precoding structure for the proposed CI-BLP method, perfect CSI is assumed throughout the paper.

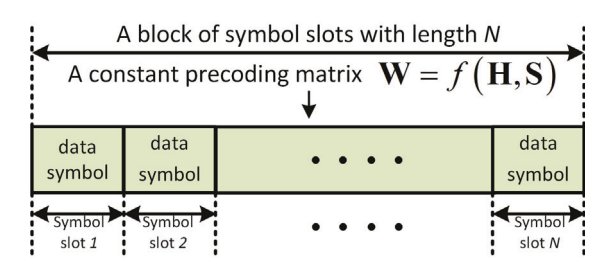


Fig. 2: The proposed CI-BLP methodology

III. PROPOSED BLOCK-LEVEL INTERFERENCE EXPLOITATION PRECODING

In this section, the proposed CI-BLP approach is introduced. As shown in Fig. 2, the proposed CI-BLP aims to exploit CI for each symbol slot simultaneously with a constant precoding matrix \mathbf{W} that is applied to all symbol slots within the block, where N is the length of the considered transmission block. In the following, we construct the optimization problem for the proposed CI-BLP method and derives its optimal precoding structure.

A. Problem Formulation

Following the principle of the 'symbol-scaling' CI metric in Fig. 1, the data symbol $\vec{OS} = s_k^n$ for user k in the n-th symbol slot and the corresponding received signal excluding noise $\vec{OB} = \mathbf{h}_L^T \mathbf{W} \mathbf{s}^n$ can be decomposed into:

$$\vec{OS} = \vec{OD} + \vec{OE} \Rightarrow s_k^n = s_{k,\mathcal{A}}^n + s_{k,\mathcal{B}}^n,$$

$$\vec{OB} = \vec{OF} + \vec{OG} \Rightarrow \mathbf{h}_k^T \mathbf{W} \mathbf{s}^n = \alpha_{k,\mathcal{A}}^n s_{k,\mathcal{A}}^n + \alpha_{k,\mathcal{B}}^n s_{k,\mathcal{B}}^n,$$
(2)

where $\alpha_{k,\mathcal{A}}^n \geq 0$ and $\alpha_{k,\mathcal{B}}^n \geq 0$ represents the scaling effect. We define $\alpha_{\mathrm{E}}^n \in \mathbb{R}^{2K}$ as

$$\boldsymbol{\alpha}_{\mathrm{E}}^{n} = \left[\alpha_{1,\mathcal{A}}^{n}, \alpha_{2,\mathcal{A}}^{n}, \cdots, \alpha_{K,\mathcal{A}}^{n}, \alpha_{1,\mathcal{B}}^{n}, \alpha_{2,\mathcal{B}}^{n}, \cdots, \alpha_{K,\mathcal{B}}^{n}\right]^{\mathrm{T}}, (3)$$

and by following the transformations in [16], $\alpha_{\rm E}^n$ can be further expressed as

$$\alpha_{\rm F}^n = \mathbf{M}^n \mathbf{W}_{\rm E} \mathbf{s}_{\rm F}^n, \tag{4}$$

where the construction of $\mathbf{M}^n \in \mathbb{R}^{2K \times 2N_T}$ directly follows Section IV-A of [16]. $\mathbf{W}_{\mathrm{E}} \in \mathbb{R}^{2N_{\mathrm{T}} \times 2K}$ and $\mathbf{s}_{\mathrm{E}}^n \in \mathbb{R}^{2K \times 1}$ in (4) are defined as

$$\mathbf{W}_{E} = \begin{bmatrix} \Re\left(\mathbf{W}\right) & -\Im\left(\mathbf{W}\right) \\ -\Im\left(\mathbf{W}\right) & \Re\left(\mathbf{W}\right) \end{bmatrix}, \ \mathbf{s}_{E}^{n} = \begin{bmatrix} \Re\left(\mathbf{s}^{n}\right)^{T}, \Im\left(\mathbf{s}^{n}\right)^{T} \end{bmatrix}^{T}.$$
(5)

From Fig. 1, we observe that a larger value of $\alpha_{k,\mathcal{A}}^n$ or $\alpha_{k,\mathcal{B}}^n$ represents a larger distance to the decision boundaries, leading to a better error-rate performance. Accordingly, the proposed CI-BLP approach aims to maximize the minimum entry in $\alpha_{\rm E}^n$ for all symbol slots within the block, and the corresponding optimization problem can be constructed as:

$$\mathcal{P}_{0}: \max_{\mathbf{W}_{E}} \min_{k,n} \alpha_{k}^{n}$$
s.t.
$$\mathbf{C1}: \alpha_{E}^{n} = \mathbf{M}^{n} \mathbf{W}_{E} \mathbf{s}_{E}^{n}, \ \forall n \leq N,$$

$$\mathbf{C2}: \sum_{n=1}^{N} \|\mathbf{W}_{E} \mathbf{s}_{E}^{n}\|_{2}^{2} \leq N p_{0},$$
(6)

$$\mathcal{L}\left(\hat{\mathbf{W}}, t, \delta_{k}^{n}, \mu\right)$$

$$= -t + \sum_{n=1}^{N} \sum_{k=1}^{2K} \delta_{k}^{n} \left[t - (\mathbf{a}_{k}^{n})^{\mathsf{T}} \hat{\mathbf{W}} \mathbf{s}_{E}^{n} - (\mathbf{b}_{k}^{n})^{\mathsf{T}} \hat{\mathbf{W}} \mathbf{c}_{E}^{n} \right] + \mu \left[\sum_{n=1}^{N} (\mathbf{s}_{E}^{n})^{\mathsf{T}} \left(\mathbf{P} \hat{\mathbf{W}} + \mathbf{Q} \hat{\mathbf{W}} \mathbf{T} \right)^{\mathsf{T}} \left(\mathbf{P} \hat{\mathbf{W}} + \mathbf{Q} \hat{\mathbf{W}} \mathbf{T} \right)^{\mathsf{T}} \mathbf{s}_{E}^{n} - N p_{0} \right]$$

$$= \left(\sum_{n=1}^{N} \mathbf{1}^{\mathsf{T}} \boldsymbol{\delta}^{n} - 1 \right) t - \sum_{n=1}^{N} (\boldsymbol{\delta}^{n})^{\mathsf{T}} \mathbf{A}^{n} \hat{\mathbf{W}} \mathbf{s}_{E}^{n} - \sum_{n=1}^{N} (\boldsymbol{\delta}^{n})^{\mathsf{T}} \mathbf{B}^{n} \hat{\mathbf{W}} \mathbf{c}_{E}^{n} + \mu \sum_{n=1}^{N} (\mathbf{s}_{E}^{n})^{\mathsf{T}} \hat{\mathbf{W}}^{\mathsf{T}} \hat{\mathbf{W}} \mathbf{s}_{E}^{n} + \mu \sum_{n=1}^{N} (\mathbf{c}_{E}^{n})^{\mathsf{T}} \hat{\mathbf{W}}^{\mathsf{T}} \hat{\mathbf{W}} \mathbf{c}_{E}^{n} - \mu N p_{0}$$

$$(14)$$

where α_k^n represents the k-th entry in α_E^n , and p_0 represents the transmit power budget per symbol slot.

 \mathcal{P}_0 is a joint optimization over all symbol slots, and it is a convex problem that can be directly solved via optimization tools such as CVX. To facilitate subsequent derivations, we introduce $\hat{\mathbf{W}}$:

$$\hat{\mathbf{W}} = \begin{bmatrix} \Re \left(\mathbf{W} \right) & -\Im \left(\mathbf{W} \right) \end{bmatrix} \in \mathbb{R}^{N_{\mathrm{T}} \times 2K}, \tag{7}$$

based on which we can decompose \mathbf{W}_{E} into

$$\mathbf{W}_{\mathrm{E}} = \mathbf{P}\hat{\mathbf{W}} + \mathbf{Q}\hat{\mathbf{W}}\mathbf{T},\tag{8}$$

where $\mathbf{P} \in \mathbb{R}^{2N_{\text{T}} \times N_{\text{T}}}$, $\mathbf{Q} \in \mathbb{R}^{2N_{\text{T}} \times N_{\text{T}}}$ and $\mathbf{T} \in \mathbb{R}^{2K \times 2K}$ are defined as

$$\mathbf{P} = \begin{bmatrix} \mathbf{I}_{N_{\mathrm{T}}} \\ \mathbf{0} \end{bmatrix}, \ \mathbf{Q} = \begin{bmatrix} \mathbf{0} \\ \mathbf{I}_{N_{\mathrm{T}}} \end{bmatrix}, \ \mathbf{T} = \begin{bmatrix} \mathbf{0} & \mathbf{I}_{K} \\ -\mathbf{I}_{K} & \mathbf{0} \end{bmatrix}. \tag{9}$$

Based on (8), the expression for $\alpha_{\rm E}^n$ is further transformed into:

$$\alpha_{E}^{n} = \mathbf{M}^{n} \mathbf{W}_{E} \mathbf{s}_{E}^{n}$$

$$= \mathbf{M}^{n} \left(\mathbf{P} \hat{\mathbf{W}} + \mathbf{Q} \hat{\mathbf{W}} \mathbf{T} \right) \mathbf{s}_{E}^{n}$$

$$= \mathbf{M}^{n} \mathbf{P} \hat{\mathbf{W}} \mathbf{s}_{E}^{n} + \mathbf{M}^{n} \mathbf{Q} \hat{\mathbf{W}} \mathbf{T} \mathbf{s}_{E}^{n}$$

$$= \mathbf{A}^{n} \hat{\mathbf{W}} \mathbf{s}_{E}^{n} + \mathbf{B}^{n} \hat{\mathbf{W}} \mathbf{c}_{E}^{n},$$
(10)

where we introduce $\mathbf{A}^n \in \mathbb{R}^{2K \times N_T}$, $\mathbf{B}^n \in \mathbb{R}^{2K \times N_T}$ and $\mathbf{c}_E^n \in \mathbb{R}^{2K \times 1}$ as

$$\mathbf{A}^n = \mathbf{M}^n \mathbf{P}, \ \mathbf{B}^n = \mathbf{M}^n \mathbf{Q}, \ \mathbf{c}_E^n = \mathbf{T} \mathbf{s}_E^n. \tag{11}$$

With the expression for the k-th entry of α_E^n given by

$$\alpha_k^n = (\mathbf{a}_k^n)^{\mathsf{T}} \hat{\mathbf{W}} \mathbf{s}_{\mathsf{E}}^n + (\mathbf{b}_k^n)^{\mathsf{T}} \hat{\mathbf{W}} \mathbf{c}_{\mathsf{E}}^n, \tag{12}$$

 \mathcal{P}_0 can be expressed in the form of a standard convex optimization problem below:

$$\mathcal{P}_{1}: \min_{\hat{\mathbf{W}},t} - t$$
s.t. $\mathbf{C1}: t - (\mathbf{a}_{k}^{n})^{\mathrm{T}} \hat{\mathbf{W}} \mathbf{s}_{\mathrm{E}}^{n} - (\mathbf{b}_{k}^{n})^{\mathrm{T}} \hat{\mathbf{W}} \mathbf{c}_{\mathrm{E}}^{n} \leq 0, \forall k \leq 2K, n \leq N,$

$$\mathbf{C2}: \sum_{n=1}^{N} \left\| \left(\mathbf{P} \hat{\mathbf{W}} + \mathbf{Q} \hat{\mathbf{W}} \mathbf{T} \right) \mathbf{s}_{\mathrm{E}}^{n} \right\|_{2}^{2} - N p_{0} \leq 0.$$
(13)

B. Closed-Form Structure for $\hat{\mathbf{W}}$

We analyze \mathcal{P}_1 based on the Lagrangian and KKT conditions to derive the optimal precoding matrix $\hat{\mathbf{W}}$. The Lagrangian of \mathcal{P}_1 can be constructed as shown in (14) on the top of this page, where $\boldsymbol{\delta}^n = \left[\delta_1^n, \delta_2^n, \cdots, \delta_{2K}^n\right]^T \in \mathbb{R}^{2K \times 1}$ and μ are the non-negative dual variables associated with the inequality constraints $\mathbf{C1}$ and $\mathbf{C2}$ respectively, where we note that

$$\mathbf{P}^{\mathsf{T}}\mathbf{P} = \mathbf{Q}^{\mathsf{T}}\mathbf{Q} = \mathbf{I}_{N_{\mathsf{T}}}, \ \mathbf{P}^{\mathsf{T}}\mathbf{Q} = \mathbf{Q}^{\mathsf{T}}\mathbf{P} = \mathbf{0}. \tag{15}$$

Accordingly, the KKT conditions for the optimality of \mathcal{P}_1 can be formulated and are shown in (16) on the top of next page. Based on the KKT conditions, we first obtain that $\mu > 0$, otherwise $\boldsymbol{\delta}^n = \mathbf{0}$, $\forall n$, which contradicts with (16a). This means that the power constraint is active when the optimality is achieved, i.e.,

$$\sum_{n=1}^{N} (\mathbf{s}_{E}^{n})^{\mathsf{T}} \hat{\mathbf{W}}^{\mathsf{T}} \hat{\mathbf{W}} \mathbf{s}_{E}^{n} + \sum_{n=1}^{N} (\mathbf{c}_{E}^{n})^{\mathsf{T}} \hat{\mathbf{W}}^{\mathsf{T}} \hat{\mathbf{W}} \mathbf{c}_{E}^{n} = N p_{0}.$$
 (17)

To proceed, we transform (16b) into

$$2\mu \hat{\mathbf{W}} \mathbf{D} = \sum_{n=1}^{N} \left[(\mathbf{A}^{n})^{\mathrm{T}} \boldsymbol{\delta}^{n} (\mathbf{s}_{\mathrm{E}}^{n})^{\mathrm{T}} + (\mathbf{B}^{n})^{\mathrm{T}} \boldsymbol{\delta}^{n} (\mathbf{c}_{\mathrm{E}}^{n})^{\mathrm{T}} \right], \quad (18)$$

where $\mathbf{D} \in \mathbb{R}^{2K \times 2K}$ is given by

$$\mathbf{D} = \left[\sum_{n=1}^{N} \mathbf{s}_{E}^{n} \left(\mathbf{s}_{E}^{n} \right)^{\mathrm{T}} + \sum_{n=1}^{N} \mathbf{c}_{E}^{n} \left(\mathbf{c}_{E}^{n} \right)^{\mathrm{T}} \right]. \tag{19}$$

Based on the fact that the block length N is in general larger than the number of users K, \mathbf{D} is thus full-rank and invertible [17]. Accordingly, we can obtain an expression for the optimal precoding matrix $\hat{\mathbf{W}}$ as a function of the Lagrange multipliers δ^n in a closed form as

$$\hat{\mathbf{W}} = \frac{1}{2\mu} \sum_{n=1}^{N} \left[(\mathbf{A}^n)^{\mathsf{T}} \boldsymbol{\delta}^n \left(\mathbf{s}_{\mathsf{E}}^n \right)^{\mathsf{T}} + (\mathbf{B}^n)^{\mathsf{T}} \boldsymbol{\delta}^n \left(\mathbf{c}_{\mathsf{E}}^n \right)^{\mathsf{T}} \right] \mathbf{D}^{-1}.$$
(20)

We observe from (20) that the expression for the optimal precoding matrix $\hat{\mathbf{W}}$ includes all the data symbols transmitted within the block. In what follows, we consider the dual problem formulation of \mathcal{P}_1 to further simplify the CI-BLP problem.

$$\frac{\partial \mathcal{L}}{\partial t} = \sum_{n=1}^{N} \mathbf{1}^{\mathrm{T}} \boldsymbol{\delta}^{n} - 1 = 0$$
 (16a)

$$\frac{\partial \mathcal{L}}{\partial \hat{\mathbf{W}}} = -\sum_{n=1}^{N} \left[\left(\boldsymbol{\delta}^{n} \right)^{\mathrm{T}} \mathbf{A}^{n} \right]^{\mathrm{T}} \left(\mathbf{s}_{\mathrm{E}}^{n} \right)^{\mathrm{T}} - \sum_{n=1}^{N} \left[\left(\boldsymbol{\delta}^{n} \right)^{\mathrm{T}} \mathbf{B}^{n} \right]^{\mathrm{T}} \left(\mathbf{c}_{\mathrm{E}}^{n} \right)^{\mathrm{T}} + 2u_{0} \hat{\mathbf{W}} \left[\sum_{n=1}^{N} \mathbf{s}_{\mathrm{E}}^{n} \left(\mathbf{s}_{\mathrm{E}}^{n} \right)^{\mathrm{T}} + \sum_{n=1}^{N} \mathbf{c}_{\mathrm{E}}^{n} \left(\mathbf{c}_{\mathrm{E}}^{n} \right)^{\mathrm{T}} \right] = \mathbf{0}$$
(16b)

$$\delta_k^n \left[t - \left(\mathbf{a}_k^n \right)^{\mathsf{T}} \hat{\mathbf{W}} \mathbf{s}_{\mathsf{E}}^n - \left(\mathbf{b}_k^n \right)^{\mathsf{T}} \hat{\mathbf{W}} \mathbf{c}_{\mathsf{E}}^n \right] = 0, \ \delta_k^n \ge 0, \ \forall k \le 2K, \ \forall n \le N$$
 (16c)

$$\mu \left[\sum_{n=1}^{N} (\mathbf{s}_{\mathrm{E}}^{n})^{\mathrm{T}} \hat{\mathbf{W}}^{\mathrm{T}} \hat{\mathbf{W}} \mathbf{s}_{\mathrm{E}}^{n} + \sum_{n=1}^{N} (\mathbf{c}_{\mathrm{E}}^{n})^{\mathrm{T}} \hat{\mathbf{W}}^{\mathrm{T}} \hat{\mathbf{W}} \mathbf{c}_{\mathrm{E}}^{n} - N p_{0} \right] = 0, \ \mu \geq 0$$
 (16d)

$$\mathcal{U} = \max_{\{\boldsymbol{\delta}^{m}\},\mu} - \sum_{m=1}^{N} (\boldsymbol{\delta}^{m})^{T} \mathbf{A}^{m} \hat{\mathbf{W}} \mathbf{s}_{E}^{m} - \sum_{m=1}^{N} (\boldsymbol{\delta}^{m})^{T} \mathbf{B}^{m} \hat{\mathbf{W}} \mathbf{c}_{E}^{m}
= \min_{\{\boldsymbol{\delta}^{m}\},\mu} \frac{1}{2\mu} \sum_{m=1}^{N} \sum_{n=1}^{N} (\boldsymbol{\delta}^{m})^{T} \mathbf{A}^{m} (\mathbf{A}^{n})^{T} \boldsymbol{\delta}^{n} (\mathbf{s}_{E}^{n})^{T} \mathbf{D}^{-1} \mathbf{s}_{E}^{m} + \frac{1}{2\mu} \sum_{m=1}^{N} \sum_{n=1}^{N} (\boldsymbol{\delta}^{m})^{T} \mathbf{A}^{m} (\mathbf{B}^{n})^{T} \boldsymbol{\delta}^{n} (\mathbf{c}_{E}^{n})^{T} \mathbf{D}^{-1} \mathbf{s}_{E}^{m}
+ \frac{1}{2\mu} \sum_{m=1}^{N} \sum_{n=1}^{N} (\boldsymbol{\delta}^{m})^{T} \mathbf{B}^{m} (\mathbf{A}^{n})^{T} \boldsymbol{\delta}^{n} (\mathbf{s}_{E}^{n})^{T} \mathbf{D}^{-1} \mathbf{c}_{E}^{m} + \frac{1}{2\mu} \sum_{m=1}^{N} \sum_{n=1}^{N} (\boldsymbol{\delta}^{m})^{T} \mathbf{B}^{m} (\mathbf{B}^{n})^{T} \boldsymbol{\delta}^{n} (\mathbf{c}_{E}^{n})^{T} \mathbf{D}^{-1} \mathbf{c}_{E}^{m}
= \min_{\{\boldsymbol{\delta}^{m}\},\mu} \frac{1}{2\mu} \sum_{m=1}^{N} \sum_{n=1}^{N} (\boldsymbol{\delta}^{m})^{T} \left[p_{m,n} \mathbf{A}^{m} (\mathbf{A}^{n})^{T} + f_{m,n} \mathbf{A}^{m} (\mathbf{B}^{n})^{T} + g_{m,n} \mathbf{B}^{m} (\mathbf{A}^{n})^{T} + q_{m,n} \mathbf{B}^{m} (\mathbf{B}^{n})^{T} \right] \boldsymbol{\delta}^{n} \tag{22}$$

C. Dual Problem Formulation

It is obvious that the Slater's condition is satisfied for the convex CI-BLP optimization problem \mathcal{P}_1 in (13) [18]. Accordingly, we can solve \mathcal{P}_1 optimally by solving its dual problem, as shown below

$$\mathcal{U} = \max_{\{\boldsymbol{\delta}^m\}, \mu} \min_{\hat{\mathbf{W}}} \mathcal{L}\left(\hat{\mathbf{W}}, t, \boldsymbol{\delta}^m, \mu\right), \tag{21}$$

where the inner minimization is achieved with (16a), the active power constraint in (17) and $\hat{\mathbf{W}}$ in (20). By substituting (16a), (17) and (20) into \mathcal{U} in (21), and by defining

$$p_{m,n} = (\mathbf{s}_{\mathsf{E}}^n)^{\mathsf{T}} \mathbf{D}^{-1} \mathbf{s}_{\mathsf{E}}^m, \ q_{m,n} = (\mathbf{c}_{\mathsf{E}}^n)^{\mathsf{T}} \mathbf{D}^{-1} \mathbf{c}_{\mathsf{E}}^m,$$

$$f_{m,n} = (\mathbf{c}_{\mathsf{F}}^n)^{\mathsf{T}} \mathbf{D}^{-1} \mathbf{s}_{\mathsf{F}}^m, \ q_{m,n} = (\mathbf{s}_{\mathsf{F}}^n)^{\mathsf{T}} \mathbf{D}^{-1} \mathbf{c}_{\mathsf{F}}^m,$$
(23)

the objective function of the dual problem \mathcal{U} can be simplified and is given by (22) above. Further defining

$$\boldsymbol{\delta}_{\mathrm{E}} = \left[\left(\boldsymbol{\delta}^{1} \right)^{\mathrm{T}}, \left(\boldsymbol{\delta}^{2} \right)^{\mathrm{T}}, \cdots, \left(\boldsymbol{\delta}^{N} \right)^{\mathrm{T}} \right]^{\mathrm{T}} \in \mathbb{R}^{2NK \times 1}$$
 (24)

and $\mathbf{U}_{m,n} \in \mathbb{R}^{2K \times 2K}$ given by

$$\mathbf{U}_{m,n} = p_{m,n} \mathbf{A}^{m} (\mathbf{A}^{n})^{\mathrm{T}} + f_{m,n} \mathbf{A}^{m} (\mathbf{B}^{n})^{\mathrm{T}} + g_{m,n} \mathbf{B}^{m} (\mathbf{A}^{n})^{\mathrm{T}} + q_{m,n} \mathbf{B}^{m} (\mathbf{B}^{n})^{\mathrm{T}},$$
(25)

the objective function of the dual problem ${\cal U}$ can finally be expressed as

$$\mathcal{U} = \min_{\{\boldsymbol{\delta}^m\}, \mu} \frac{1}{2\mu} \left(\boldsymbol{\delta}_{\mathrm{E}}\right)^{\mathrm{T}} \mathbf{U} \boldsymbol{\delta}_{\mathrm{E}}, \tag{26}$$

where $\mathbf{U} \in \mathbb{R}^{2NK \times 2NK}$ is a block matrix constructed as

$$\mathbf{U} = \begin{bmatrix} \mathbf{U}_{1,1} & \cdots & \cdots & \mathbf{U}_{1,N} \\ \vdots & \ddots & \mathbf{U}_{m,n} & \ddots & \vdots \\ \mathbf{U}_{N,1} & \cdots & \cdots & \mathbf{U}_{N,N} \end{bmatrix}. \tag{27}$$

In the following, we simplify the block-level power constraint in (17). By substituting the expression for $\hat{\mathbf{W}}$ in (20) into (17), the first term on the left-hand side of (17) is expanded and shown in (28) on the top of next page. Based on the result in (28) and by introducing $\mathbf{F}_{m,n}^l \in \mathbb{R}^{2K \times 2K}$ as

$$\mathbf{F}_{m,n}^{l} = p_{l,n} p_{m,l} \mathbf{A}^{m} \left(\mathbf{A}^{n}\right)^{\mathsf{T}} + f_{l,n} p_{m,l} \mathbf{A}^{m} \left(\mathbf{B}^{n}\right)^{\mathsf{T}} + p_{l,n} g_{m,l} \mathbf{B}^{m} \left(\mathbf{A}^{n}\right)^{\mathsf{T}} + f_{l,n} g_{m,l} \mathbf{B}^{m} \left(\mathbf{B}^{n}\right)^{\mathsf{T}},$$
(29)

the first term on the left-hand side of (17) can finally be expressed in a compact form as

$$\sum_{l=1}^{N} (\mathbf{s}_{E}^{l})^{\mathrm{T}} \hat{\mathbf{W}}^{\mathrm{T}} \hat{\mathbf{W}} \mathbf{s}_{E}^{l} = \frac{1}{4\mu^{2}} (\boldsymbol{\delta}_{E})^{\mathrm{T}} \mathbf{F} \boldsymbol{\delta}_{E},$$
(30)

where $\mathbf{F} = \sum_{l=1}^{N} \mathbf{F}^{l} \in \mathbb{R}^{2NK \times 2NK}$, with each \mathbf{F}^{l} being a block matrix constructed with $\mathbf{F}_{m,n}^{l}$ similarly to the construction of \mathbf{U} in (27).

Following the above procedure, the second term on the lefthand side of (17) can be similarly expressed in a compact form

$$\sum_{n=1}^{N} (\mathbf{c}_{E}^{n})^{T} \hat{\mathbf{W}}^{T} \hat{\mathbf{W}} \mathbf{c}_{E}^{n} = \frac{1}{4\mu^{2}} (\boldsymbol{\delta}_{E})^{T} \mathbf{G} \boldsymbol{\delta}_{E},$$
(31)

$$\sum_{l=1}^{N} \left(\mathbf{s}_{E}^{l}\right)^{\mathsf{T}} \hat{\mathbf{W}}^{\mathsf{T}} \hat{\mathbf{W}} \mathbf{s}_{E}^{l}$$

$$= \frac{1}{4\mu^{2}} \sum_{l=1}^{N} \left(\mathbf{s}_{E}^{l}\right)^{\mathsf{T}} \left\{ \sum_{m=1}^{N} \left[\left(\mathbf{A}^{m}\right)^{\mathsf{T}} \boldsymbol{\delta}^{m} \left(\mathbf{s}_{E}^{m}\right)^{\mathsf{T}} + \left(\mathbf{B}^{m}\right)^{\mathsf{T}} \boldsymbol{\delta}^{m} \left(\mathbf{c}_{E}^{m}\right)^{\mathsf{T}} \right] \mathbf{D}^{-1} \right\}^{\mathsf{T}} \left\{ \sum_{n=1}^{N} \left[\left(\mathbf{A}^{n}\right)^{\mathsf{T}} \boldsymbol{\delta}^{n} \left(\mathbf{s}_{E}^{n}\right)^{\mathsf{T}} + \left(\mathbf{B}^{n}\right)^{\mathsf{T}} \boldsymbol{\delta}^{n} \left(\mathbf{c}_{E}^{n}\right)^{\mathsf{T}} \right] \mathbf{D}^{-1} \right\} \mathbf{s}_{E}^{l}$$

$$= \frac{1}{4\mu^{2}} \sum_{l=1}^{N} \sum_{m=1}^{N} \sum_{n=1}^{N} \left\{ \left(\boldsymbol{\delta}^{m}\right)^{\mathsf{T}} \left[p_{l,n} p_{m,l} \mathbf{A}^{m} \left(\mathbf{A}^{n}\right)^{\mathsf{T}} + f_{l,n} p_{m,l} \mathbf{A}^{m} \left(\mathbf{B}^{n}\right)^{\mathsf{T}} + p_{l,n} g_{m,l} \mathbf{B}^{m} \left(\mathbf{A}^{n}\right)^{\mathsf{T}} + f_{l,n} g_{m,l} \mathbf{B}^{m} \left(\mathbf{B}^{n}\right)^{\mathsf{T}} \right] \boldsymbol{\delta}^{n} \right\}$$
(28)

where $\mathbf{G} = \sum_{l=1}^{N} \mathbf{G}^{l}$. Each $\mathbf{G}^{l} \in \mathbb{R}^{2NK \times 2NK}$, $\forall l \leq N$ is formulated with $\mathbf{G}^{l}_{m,n}$ similarly to the construction of \mathbf{U} in (27), where $\mathbf{G}^{l}_{m,n} \in \mathbb{R}^{2K \times 2K}$ is given by

$$\mathbf{G}_{m,n}^{l} = g_{l,n} f_{m,l} \mathbf{A}^{m} \left(\mathbf{A}^{n}\right)^{\mathrm{T}} + q_{l,n} f_{m,l} \mathbf{A}^{m} \left(\mathbf{B}^{n}\right)^{\mathrm{T}} + g_{l,n} q_{m,l} \mathbf{B}^{m} \left(\mathbf{A}^{n}\right)^{\mathrm{T}} + q_{l,n} q_{m,l} \mathbf{B}^{m} \left(\mathbf{B}^{n}\right)^{\mathrm{T}}.$$
(32)

Based on the above derivations, the block-level power constraint (17) is equivalent to:

$$\frac{1}{4\mu^{2}} (\boldsymbol{\delta}_{E})^{T} \mathbf{F} \boldsymbol{\delta}_{E} + \frac{1}{4\mu^{2}} (\boldsymbol{\delta}_{E})^{T} \mathbf{G} \boldsymbol{\delta}_{E} = N p_{0}$$

$$\Rightarrow \frac{1}{4\mu^{2}} (\boldsymbol{\delta}_{E})^{T} (\mathbf{F} + \mathbf{G}) \boldsymbol{\delta}_{E} = N p_{0}.$$
(33)

By studying the relationship between (F + G) and U, we arrive at the following proposition.

Proposition 1: F, G, and U satisfy the following condition:

$$\mathbf{F} + \mathbf{G} = \mathbf{U}.\tag{34}$$

Proof: This proposition can be proved by expressing the generic (m, n)-th block in $(\mathbf{F} + \mathbf{G})$ and \mathbf{U} , and through some mathematical transformations we can obtain $\mathbf{F}_{m,n} + \mathbf{G}_{m,n} = \mathbf{U}_{m,n}$, which completes the proof.

According to **Proposition 1** and based on the block-level power constraint in (33), we can obtain the following expression for μ :

$$\frac{1}{4\mu^2} \left(\boldsymbol{\delta}_{\mathrm{E}} \right)^{\mathrm{T}} \mathbf{U} \boldsymbol{\delta}_{\mathrm{E}} = N p_0 \ \Rightarrow \ \mu = \sqrt{\frac{\left(\boldsymbol{\delta}_{\mathrm{E}} \right)^{\mathrm{T}} \mathbf{U} \boldsymbol{\delta}_{\mathrm{E}}}{4N p_0}}. \tag{35}$$

Substituting the above expression for u_0 into (26), \mathcal{U} can be transformed into an optimization on δ_E only, given by

$$\mathcal{U} = \min_{\boldsymbol{\delta}_{E}, \mu} \frac{1}{2\mu} \boldsymbol{\delta}_{E}^{T} \mathbf{U} \boldsymbol{\delta}_{E}$$

$$= \min_{\boldsymbol{\delta}_{E}} \frac{1}{2\sqrt{\frac{(\boldsymbol{\delta}_{E})^{T} \mathbf{U} \boldsymbol{\delta}_{E}}{4Np_{0}}}} \boldsymbol{\delta}_{E}^{T} \mathbf{U} \boldsymbol{\delta}_{E}$$

$$= \min_{\boldsymbol{\delta}_{E}} \sqrt{Np_{0} \boldsymbol{\delta}_{E}^{T} \mathbf{U} \boldsymbol{\delta}_{E}}$$

$$= \min_{\boldsymbol{\delta}_{E}} \boldsymbol{\delta}_{E}^{T} \mathbf{U} \boldsymbol{\delta}_{E},$$
(36)

where the last step is achieved because $y = \sqrt{x}$ is a monotonic function. Accordingly, the final dual problem of the proposed

CI-BLP optimization for PSK modulation can be formulated as

$$\mathcal{P}_{2}: \min_{\boldsymbol{\delta}_{E}} \boldsymbol{\delta}_{E}^{T} \mathbf{U} \boldsymbol{\delta}_{E}$$
s.t. $\mathbf{C}\mathbf{1}: \mathbf{1}^{T} \boldsymbol{\delta}_{E} - 1 = 0,$ (37)
$$\mathbf{C}\mathbf{2}: \boldsymbol{\delta}_{E}^{m} \geq 0, \ \forall m \in \{1, 2, \cdots, 2NK\},$$

 \mathcal{P}_2 is a QP optimization problem over a simplex, which can be more efficiently solved than the original CI-BLP optimization problem \mathcal{P}_1 via the standard simplex method [19], [20] or the interior-point methods [21]. After solving \mathcal{P}_2 and obtaining $\hat{\mathbf{W}}$ via (20), the original complex precoding matrix \mathbf{W} in (1) can be obtained by

$$\mathbf{W} = \hat{\mathbf{W}}\hat{\mathbf{P}} - \jmath\hat{\mathbf{W}}\hat{\mathbf{Q}},\tag{38}$$

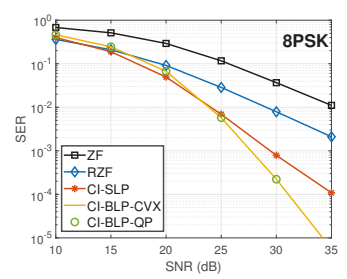
where the form of $\hat{\mathbf{P}}$ and $\hat{\mathbf{Q}}$ follows (9) while their dimension is changed into $2K \times K$.

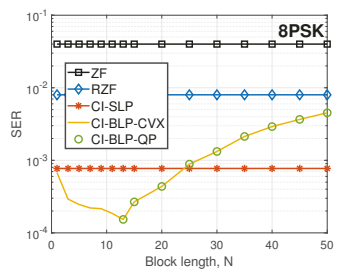
IV. NUMERICAL RESULTS

We present numerical results to validate our above derivations and illustrate the superiority of the proposed CI-BLP approach. Throughout the simulations, $K=N_{\rm T}=12$, and 8PSK modulation is employed. The transmit power budget per symbol slot is set as $p_0=1$, leading to the total transmit power budget for the considered block of symbol slots as $P_{\rm total}=Np_0=N$. We compare CI-BLP with block-level ZF-based precoding and traditional CI-SLP under standard Rayleigh fading channels.

Fig. 3 depicts the symbol-error rate (SER) performance of different BLP and SLP approaches, where the block length is N=15. Compared with BLP approaches (ZF/RZF), CI-based precoding methods achieve an improved SER performance by exploiting CI. Thanks to the relaxed block-level power constraint, the CI-BLP method proposed in this paper offers additional performance improvements over traditional CI-SLP methods in the literature with reduced computational costs, making CI-BLP more attractive in practical MIMO communication systems. The results in Fig. 3 also validate the correctness of our derivations in the paper.

Fig. 4 presents the SER performance of the proposed CI-BLP scheme with respect to the block length N, where the transmit SNR is fixed at 30dB. The block length N does not affect the design of ZF, RZF and traditional CI-SLP precoding,





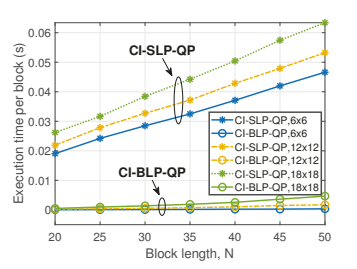


Fig. 3 SER v.s. SNR, N=15

Fig. 4 SER v.s. block length N

Fig. 5 Execution time v.s. block length N

Numerical comparisons for the proposed CI-BLP approach, 8PSK, $K=N_{\rm T}=12$

resulting in constant SER results. Interestingly, as the block length N increases, CI-BLP's SER performance first improves thanks to the relaxed power constraint, which outweighs the loss due to using a constant precoding matrix over the block. As N further increases, the SER performance becomes worse because relaxed power constraint cannot further compensate for the loss of using a constant precoding matrix.

Fig. 5 evaluates the computational complexity gain of the proposed CI-BLP method over traditional CI-SLP in terms of the execution time, where results for 6×6 , 12×12 and 18×18 MU-MISO systems are presented. For fairness of comparison, only the execution time required for running the 'quadprog' function in MATLAB used to solve the QP problem for both CI-BLP and CI-SLP is evaluated. We observe from Fig. 5 that the proposed CI-BLP approach offers a significant complexity gain over traditional CI-SLP, and the complexity gains become more prominent as the block length N increases.

V. CONCLUSIONS

A block-level interference exploitation precoding termed CI-BLP is proposed for downlink MU-MISO, where a constant precoding matrix is applied to a block of data symbols, thus removing the symbol-by-symbol optimization required in traditional SLP. The proposed CI-BLP optimization problem is shown to be equivalent to a QP problem over a simplex. Thanks to the relaxed block-level power constraint, a superior performance for the proposed CI-BLP scheme over traditional CI-SLP precoding is observed when the length of the symbol slots is short, while only a slight performance loss is exhibited as the length of the symbol slots increases, as validated by the numerical results.

REFERENCES

- [1] T. Haustein, C. von Helmolt, E. Jorswieck, V. Jungnickel, and V. Pohl, "Performance of MIMO Systems with Channel Inversion," in Vehicular Technology Conference. IEEE 55th Vehicular Technology Conference. VTC Spring 2002 (Cat. No.02CH37367), vol. 1, 2002, pp. 35–39.
- [2] Q. H. Spencer, A. L. Swindlehurst, and M. Haardt, "Zero-Forcing Methods for Downlink Spatial Multiplexing in Multiuser MIMO Channels," *IEEE Trans. Commun.*, vol. 52, no. 2, pp. 461–471, Feb. 2004.
- [3] C. B. Peel, B. M. Hochwald, and A. L. Swindlehurst, "A Vector-Perturbation Technique for Near-Capacity Multiantenna Multiuser Communication-part I: Channel Inversion and Regularization," *IEEE Trans. Commun.*, vol. 53, no. 1, pp. 195–202, Jan. 2005.
- [4] A. Wiesel, Y. C. Eldar, and S. Shamai (Shitz), "Linear Precoding via Conic Optimization for Fixed MIMO Receivers," *IEEE Trans. Sig. Process.*, vol. 54, no. 1, pp. 161–176, Jan. 2006.

- [5] F. Wang, X. Wang, and Y. Zhu, "Transmit Beamforming for Multiuser Downlink with Per-Antenna Power Constraints," in 2014 IEEE International Conference on Communications (ICC), Sydney, NSW, 2014, pp. 4692–4697.
- [6] S. S. Christensen, R. Agarwal, E. De Carvalho, and J. M. Cioffi, "Weighted sum-rate maximization using weighted MMSE for MIMO-BC beamforming design," *IEEE Trans. Wireless Commun.*, vol. 7, no. 12, pp. 4792–4799, Dec. 2008.
- [7] A. Li, D. Spano, J. Krivochiza, S. Domouchtsidis, C. G. Tsinos, C. Masouros, S. Chatzinotas, Y. Li, B. Vucetic, and B. Ottersten, "A Tutorial on Interference Exploitation via Symbol-Level Precoding: Overview, State-of-the-Art and Future Directions," *IEEE Commun. Sur. & Tut.*, vol. 22, no. 2, pp. 796–839, secondquarter 2020.
- [8] M. Alodeh, D. Spano, A. Kalantari, C. G. Tsinos, D. Christopoulos, S. Chatzinotas, and B. Ottersten, "Symbol-Level and Multicast Precoding for Multiuser Multiantenna Downlink: A State-of-the-Art, Classification, and Challenges," *IEEE Commun. Sur. & Tut.*, vol. 20, no. 3, pp. 1733–1757, thirdquarter 2018.
- [9] C. Masouros and G. Zheng, "Exploiting Known Interference as Green Signal Power for Downlink Beamforming Optimization," *IEEE Trans. Sig. Process.*, vol. 63, no. 14, pp. 3628–3640, July 2015.
- [10] A. Li and C. Masouros, "Interference Exploitation Precoding Made Practical: Optimal Closed-Form Solutions for PSK Modulations," *IEEE Trans. Wireless Commun.*, vol. 17, no. 11, pp. 7661–7676, Nov. 2018.
- [11] A. Haqiqatnejad, F. Kayhan, and B. Ottersten, "Power Minimizer Symbol-Level Precoding: A Closed-Form Suboptimal Solution," *IEEE Sig. Process. Lett.*, vol. 25, no. 11, pp. 1730–1734, Nov. 2018.
- [12] D. Spano, M. Alodeh, S. Chatzinotas, and B. Ottersten, "Faster-Than-Nyquist Signaling Through Spatio-Temporal Symbol-Level Precoding for the Multiuser MISO Downlink Channel," *IEEE Trans. Wireless Commun.*, vol. 17, no. 9, pp. 5915–5928, Sept. 2018.
- Commun., vol. 17, no. 9, pp. 5915–5928, Sept. 2018.
 [13] Y. Liu, M. Shao, W.-K. Ma, and Q. Li, "Symbol-Level Precoding Through the Lens of Zero Forcing and Vector Perturbation," *IEEE Trans. Sig. Process.*, vol. 70, pp. 1687–1703, 2022.
- [14] A. Mohammad, C. Masouros, and Y. Andreopoulos, "An Unsupervised Learning-Based Approach for Symbol-Level-Precoding," in 2020 IEEE Global Communications Conference (GLOBECOM 2020), 2021.
- [15] A. Li, C. Masouros, Y. Li, B. Vucetic, and A. L. Swindlehurst, "Interference Exploitation Precoding for Multi-Level Modulations: Closed-Form Solutions," *IEEE Trans. Commun.*, vol. 69, no. 1, pp. 291–308, Jan. 2021.
- [16] A. Li, C. Masouros, F. Liu, and A. L. Swindlehurst, "Massive MIMO 1-Bit DAC Transmission: A Low-Complexity Symbol Scaling Approach," *IEEE Trans. Wireless Commun.*, vol. 17, no. 11, pp. 7559–7575, Nov. 2018
- [17] 3GPP TR 21.916, "Technical Specification Group Services and System Aspects," Release 16, 2022, Version 16.1.0.
- [18] L. Vandenberghe and S. Boyd, Convex Optimization. Cambridge University Press, 2004.
- [19] P. Wolfe, "The Simplex Method for Quadratic Programming," *Econometrica*, vol. 27, no. 3, pp. 382–398, July 1959.
- [20] G. Cornuejols and R. Tutuncu, Optimization Methods in Finance. Cambridge University Press, Dec. 2006.
- [21] F. Alizadeh and D. Goldfarb, "Second-Order Cone Programming," Mathematical Programming, vol. 95, no. 1, pp. 3–51, 2003.